Biology Direct

RESEARCH

Open Access

# Mechanism of LINC01018/miR-182-5p/Rab27B in the immune escape through PD-L1-mediated CD8$^+$ T cell suppression in glioma

Su Hu[1†], Guoshuo Chen[2†], Aiping Luo[3†], Hailin Zhao[1], Dan Li[1], Biao Peng[1*], Jike Du[4*] and Dongdong Luo[1*]

## Abstract

**Background** Glioma is a malignant tumor associated with poorer prognosis. This study aims to elucidate the mechanism of LINC01018/miR-182-5p/Rab27B axis in PD-L1-mediated CD8$^+$ T cell suppression in the progression of gliomas.

**Methods** LINC01018, miR-182-5p, and Rab27B expression levels in glioblastoma tissues were measured. The proportion of infiltrating macrophages and monocytes and CD8$^+$ T cell function were assessed. The relationship between miR-182-5p and Rab27B was analyzed. Glioma cell activity, invasion, and migration were measured. The expression of E-cadherin, N-cadherin, Vimentin, PD-L1, iNOS, and CD206 was determined. Glioma cell-derived EVs were isolated, and the co-localization of Rab27B and PD-L1 and the binding of Rab27B to PD-L1 were analyzed. The endocytosis of EVs by microglia was assayed. The impact of LINC01018/miR-182-5p/Rab27B on glioma growth was observed. The function of macrophages and CD8$^+$ T cells in tumors was analyzed.

**Results** Rab27B was downregulated, and infiltrating macrophages and monocytes were increased in glioblastoma. miR-182-5p inhibited Rab27B expression. Rab27B knockdown reverses the inhibitory effect of LINC01018 overexpression on glioma cell growth. Glioma cells-derived EVs with low Rab27B expression carried more PD-L1 to increase PD-L1 expression and M2 polarization in microglia. LINC01018 overexpression reduced macrophages in orthotopic tumors. CD8$^+$ T cell numbers showed no significant difference, but TIM-3 increased and IFN-γ decreased. miR-182-5p inhibition enhanced the therapeutic effect of anti-PD-L1, which was reversed after glioma cell-derived EVs.

**Conclusion** LINC01018 promotes PD-L1-mediated CD8$^+$ T cell suppression via the miR-182-5p/Rab27B axis in glioma cell-derived EVs, thereby contributing to immune escape in gliomas.

†Su Hu, Guoshuo Chen and Aiping Luo contributed equally to this work.

*Correspondence:
Biao Peng
cebt01@163.com
Jike Du
dnlxzv@163.com
Dongdong Luo
Luodongdong1242@163.com

Full list of author information is available at the end of the article

**Keywords** Glioma, Immune escape, LINC01018, miR-182-5p, Rab27B, EVs

## Introduction

Glioma is a common primary tumor found in the brain and spinal cord, typically originating from glial cells or precursor cells [1]. Gliomas are classified into four grades, and higher grades are associated with poorer prognosis, and the median overall survival time reduces from 11.6 years in patients with low-grade glioma to 15 months in patients with grade 4 glioma [2]. The standard treatment for gliomas involves surgical resection of the tumor followed by adjuvant radiotherapy and chemotherapy; however, the therapeutic efficacy of glioma is widely limited by factors such as tumor immune escape and the complex tumor microenvironment [3]. Notably, gliomas contain a large number of glioma-associated microglia/macrophages, which promote an immunosuppressive microenvironment and facilitate glioma progression [4]. Thus, our study centered on the mechanisms of immune evasion in gliomas, providing new theoretical insights that may contribute to the development of therapeutic methods for glioma.

Long non-coding RNAs (lncRNAs) are defined as RNA transcripts longer than 200 nucleotides that do not encode proteins and function as regulatory units [5]. LncRNAs regulate mechanisms of cell death and tumor metastasis by targeting microRNAs (miRNAs) in cancers, thereby exerting oncogenic or tumor-suppressive functions [6]. Of note, LINC01018 is involved in glioma tumor growth and the malignant phenotype of glioma cells in mice [7]. Our preliminary study has confirmed that the LINC01018/miR-182-5p axis inhibits glioma cell growth [8]. However, their downstream genes and their effects on immune evasion in gliomas remain to be further elucidated.

The member RAS oncogene family (Rab27B) is a small RAB GTPase that regulates the exocytosis of various vesicles in multicellular organisms [9]. Here, database predictions have indicated that miR-182-5p targets Rab27B, which may be a potential key factor in the development and progression of gliomas. Rab27B is a direct regulator protein for the transport of extracellular vesicles (EVs) to the plasma membrane [10]. Notably, cancer cell-derived-EVs carry aberrantly overexpressed or mutated proteins and other biomolecules, sharing oncogenic material [11]. More importantly, a recent report has found that Rab27B is upregulated in metformin-treated glioma cells, along with decreased cell survival [12].

Programmed death ligand 1 (PD-L1), an I-type transmembrane protein belonging to the immunoglobulin (Ig) superfamily, inhibits T-cell activation signals by binding to its receptor PD-1 on activated T cells, thereby suppressing antitumor immunity [13]. Blocking the PD-1/PD-L1 pathway allows for the effective delivery of activation signals to downstream proteins and signaling pathways, ultimately stimulating T-cell proliferation and differentiation, and preventing the immune escape of tumor cells [14]. Tumor-associated macrophages (TAMs) upregulate PD-L1 expression in tumor cells and induce T cell suppression, thus promoting the development of the tumor microenvironment [15]. A previous study has shown that Rab27B inhibition promotes the delivery of PD-L1 into EVs, which are transferred to TAMs, exacerbating the suppression of $CD8^+$ T cells in hepatocellular carcinoma [10]. We hypothesize that Rab27B inhibition can activate PD-L1 function and thus promote immune evasion in glioma.

Based on our previous research, we explored the specific mechanism by which the LINC01018/miR-182-5p/Rab27B axis promotes the delivery of PD-L1 via EVs from glioma cells to microglia, thereby mediating immune evasion. This investigation aims to provide new theoretical insights for the treatment of glioma.

## Materials and methods

### Ethics statement

The study protocol adhered to the ethical guidelines of ethics committee of Guangzhou Institute of Cancer Research, the Affiliated Cancer Hospital, Guangzhou Medical University and the Declaration of Helsinki. All animal experiments were approved by the ethics committee of Guangzhou Institute of Cancer Research, the Affiliated Cancer Hospital, Guangzhou Medical University and conducted in accordance with the Guide for the Care and Use of Laboratory Animals [16].

### Clinical sample collection

This study included glioma tissues and adjacent normal tissues from 78 glioblastoma patients who underwent surgical resection at Guangzhou Institute of Cancer Research, the Affiliated Cancer Hospital, Guangzhou Medical University between 2015 and 2022. Informed consent forms were collected from all participants.

### Cell culture

Normal human astrocytes (NHA), human glioma cell lines (U251, T98G, LN229, A172), and the mouse glioma cell line (GL261) were garnered from the Shanghai Institute of Biological Sciences, Chinese Academy of Sciences (Shanghai, China). The human microglial cell line (HMC3) was purchased from ATCC (Manassas, VA, USA). NHAs were cultured in RPMI-1640 medium (Invitrogen, Carlsbad, CA, USA) supplemented with 10% fetal bovine serum (FBS; GIBCO, Grand Island, NY, USA).

Microglial cells and glioma cell lines were cultured in Dulbecco's modified Eagle medium (Invitrogen) at 37 °C and 5% $CO_2$. Mycoplasma contamination was routinely monitored using a mycoplasma polymerase chain reaction (PCR) detection kit (Biosmart).

## Cell treatment

The full-length sequences of LINC01018 and Rab27B complementary DNA (cDNA) were synthesized and cloned into the pcDNA3.0 vector (Invitrogen) to generate pc-LINC01018 and pc-Rab27B constructs. Cre was cloned into the pc-Rab27B vector to obtain Rab27B-Cre fusion protein. The plasmid pLV-CMV-LoxP-DsRed-LoxP-eGFP was obtained from Addgene (#65726, Watertown, MA, USA). Hsa-miR-182-5p mimics (mimic-182-5p) and their controls (mimic-NC), sh-Rab27B, and control sh-NC were synthesized by Sangon Biotech (Shanghai, China). Lipofectamine 3000 (Invitrogen) was used to transfect the LINC01018 plasmid (pc-LINC01018), Rab27B plasmid (pc-Rab27B), miR-182-5p mimic, and sh-Rab27B into glioma cells.

To establish stable glioma and microglial cell lines via lentiviral infection, lentiviral plasmids were co-transfected with psPAX2 and pMD2 into HEK293T cells to produce lentivirus. The G vector was transfected using Fugene (Promega, Madison, WI, USA) following the manufacturer's instructions. After 48 h, viral supernatants were harvested, filtered through a 0.45 mm filter, and prepared to infect glioma cells or microglia. The stable cell lines were obtained by screening with 3 μg/mL puromycin for one week. Ultimately, stable HMC3 cells for Cre-LoxP experiments were obtained. U251 and T98G cells with stable overexpression of LINC01018 (Lv-LINC01018) and control (Lv-NC) and GL261 cells with stable low expression of miR-182-5p (Lv-antagomiR) and control (Lv-NC) were obtained for in vivo tumorigenesis experiments.

## Flow cytometry

Tumor-infiltrating cells were prepared using a gentle MACSTM Dissociator and a tumor dissociation kit (Miltenyi Biotec, Auburn, CA, USA) following the manufacturer's instructions. The isolated cells were subjected to surface and intracellular flow cytometry staining and analyzed on a Cytoflex flow cytometer (Beckman Coulter Life Sciences, Miami, FL, USA). In brief, the cells were incubated in Fc-block and then stained with antibodies. Cell Stimulation Cocktail (eBioscience™, San Diego, CA, USA) was used to stimulate the cells for 4 h, followed by intracellular cytokine staining.

For surface staining, cells were washed and incubated with antibodies for 30 min at 4 °C. For intracellular staining, samples were fixed and permeabilized using Cytofix/Cytoperm kit (BD Biosciences, San Jose, CA, USA) or Transcription Factor Buffer Set (BD Biosciences) and incubated with intracellular antibodies for 30–45 min at 4 °C. Dead cells were stained with Fixable Viability Dye 780 (BD Biosciences). IgG served as a negative control. Flow cytometry data were analyzed using FlowJo. Antibodies used for flow cytometry were as follows: PerCP/Cy5.5®-mouse anti-human CD45 (ab157309, Abcam, Cambridge, MA, USA), PerCP/Cy5.5®-rabbit anti-mouse CD45 (ab210342, Abcam), Alexa Fluor® 647-rabbit anti-human CD14 (ab302698, Abcam), Alexa Fluor® 488-mouse anti-human CD68 (ab222914, Abcam), FITC-mouse anti-human CD3 (ab34275, Abcam), APC-mouse anti-human CD8 (ab26004, Abcam), APC-rabbit anti-mouse CD8 (ab237368, Abcam), eFluor™ 450-rabbit anti-mouse T-cell immunoglobulin and mucin domain-3 (TIM-3) (48-5871-82, Invitrogen), Super Bright™ 436-mouse anti-human TIM-3 (62-3109-42, Invitrogen), eFluor™ 450-mouse anti-human interferon-γ (IFN-γ) (48-7319-42, Invitrogen), eFluor™ 450-rabbit anti-mouse IFN-γ (48-7311-82, Invitrogen), Alexa Fluor® 488-rabbit anti-mouse F4/80 (ab237331, Abcam), eFluor™ 450-Rat anti-mouse CD206 (48-2061-82, Invitrogen), and APC-Rat anti-mouse CD11b (ab25482, Abcam).

### Quantitative real-time polymerase chain reaction (qRT-PCR)

Total RNA was isolated from tissue samples and cells using TRIzol reagent (Invitrogen) and reverse transcribed into cDNA using Primescript reverse transcriptase (Takara, Dalian, China) according to the manufacturer's instructions. Target gene expression was quantified by RT-qPCR using PrimeScript RT-PCR kit (Takara) or TaqMan MicroRNA assays (Applied Biosystems, Carlsbad, CA, USA). Relative expression was normalized to the internal control glyceraldehyde-phosphate dehydrogenase (GAPDH) or U6 [17]. For calculation of the relative expression levels of the products, the $2^{-\Delta\Delta Ct}$ method was employed [18]. Primer sequences used for qRT-PCR are shown in Table 1.

## Western blot assay

Glioma cells or homogenized tissues were lysed in ice-cold radioimmunoprecipitation assay buffer (Beyotime, Shanghai, China). Equal amounts of protein extracts were separated by sodium dodecyl sulfate polyacrylamide gel electrophoresis (SDS-PAGE) and then transferred onto polyvinylidene fluoride membranes. The membranes were blocked with a 10% bovine serum albumin solution to prevent non-specific antibody binding, and then incubated with the primary antibodies as follows: Rab27B (1:1000, ab317264, Abcam), PD-L1 (1:1000, PA5-20343, Invitrogen), E-Cadherin (1:1000, ab231303, Abcam), N-Cadherin (1:5000, ab76011, Abcam), Vimentin (1:3000, ab92547, Abcam), iNOS (1:1000, ab178945,

**Table 1** PCR primer sequences

| Gene | Sequences (5′-3′) |
|---|---|
| LINC01018 (human) | F: CTTCCAGGTGGCAGAGGAGAGG |
| | R: TCGTCCAAAGCGGTTTCCAAAGG |
| hsa-miR-182-5p | F: GCCGAGTTTGGCAATGGTAG |
| | R: CTCAACTGGTGTCGTGGA |
| mmu-miR-182-5p | F: GCCGAGTTTGGCAATGGTAGA |
| | R: CTCAACTGGTGTCGTGGA |
| Rab27B (human) | F: TAGACTTTCGGGAAAAACGTGTG |
| | R: AGAAGCTCTGTTGACTGGTGA |
| Rab27B (mouse) | F: CGTCAGGAAAAGCGTTTAAGGT |
| | R: AGAAGCTCTGTTGACTGGTGA |
| GAPDH (human) | F: GGAGCGAGATCCCTCCAAAAT |
| | R: GGCTGTTGTCATACTTCTCATGG |
| GAPDH (mouse) | F: AGGTCGGTGTGAACGGATTTG |
| | R: TGTAGACCATGTAGTTGAGGTCA |
| U6 (human) | F: TCGCTTCGGCAGCACATATACT |
| | R: AGGTGGCTTTGGTGGAAGAG |
| U6 (mouse) | F: ATGGCGGACGACGTAGATCAGCA |
| | R:TCAGCCAACTCTCAATGGAGGGG |

Abcam), CD206 (1:2000, ab64693, Abcam), and β-actin (1:2000, ab8227, Abcam). Protein bands were visualized using an enhanced chemiluminescence kit (Beyotime). The grayscale values were analyzed with β-actin serving as the internal control to determine the relative expression levels of the target proteins.

## Cell counting kit-8 (CCK-8) assay

The CCK-8 (Dojindo, Kumamoto, Japan) assay was conducted to evaluate cell viability at designated intervals (24, 48, 72, and 96 h). The optical density values were measured using a microplate spectrophotometer.

### Transwell assay

Transwell chambers (Corning, NY, USA) with 8 μm pore size, either uncoated or precoated with Matrigel (BD, San Diego, CA, USA), were utilized for the assessment of cell migration and invasion. Glioma cells were collected and suspended in a serum-free medium. The cell suspensions were supplemented to the upper chamber, while a complete medium supplemented with 20% FBS was applied to the lower chamber. Non-migrated or non-invaded cells were removed after incubation. The remaining cells were fixed and stained with crystal violet. The number of migrated or invaded cells was counted from five randomly selected fields using a microscope.

For co-culture experiments, glioma cells were added to the upper chamber of the Transwell with or without GW4869 treatment, while HMC3 cells were placed in the lower chamber. After co-culturing for 48 h, PD-L1 expression in HMC3 cells in the lower chamber was detected.

### Dual-luciferase reporter assay

Cells were transfected with pmirGLO-Rab27B-WT or pmirGLO-Rab27B-MUT plasmids along with miR-182-5p mimics (miR-mimic) or negative control mimics (mimic-NC) using Lipofectamine 2000. Relative luciferase activity was measured using the dual-luciferase reporter assay system (Promega) according to the manufacturer's instructions.

### EV isolation and characterization

At 90% confluence, cells were washed with phosphate-buffered saline (PBS), followed by a 48-hour incubation in a serum-free medium to allow EV release. Afterward, the supernatant was garnered and centrifuged at 300 g for 10 min, followed by centrifugation at 3000 g for 20 min at 4 °C to remove cells and apoptotic bodies. The supernatant was then filtered through a 0.22 μm filter to eliminate cellular debris. Subsequently, the filtered supernatant was transferred to Amicon Ultra-15 centrifugal filter units with a molecular weight cutoff of 100 kDa (Millipore, Billerica, MA, USA). The ultrafiltration liquid was centrifuged at 4000 g for 30 min, and the supernatant was mixed with EV precipitation solution (ExoFast-TX, System Biosciences, San Francisco Bay Area, CA, USA) and incubated overnight at 4 °C. Afterward, the samples were centrifuged at 1500 g for 30 min at 4 °C to obtain the final particles. The final pellets containing EVs were resuspended in PBS for subsequent analysis. The total EV protein concentration was determined using a bicinchoninic acid (BCA) kit (Thermo Fisher Scientific, Waltham, MA, USA).

The size, distribution, and concentration of EVs were measured using a ZetaView nanoparticle tracking analyzer (NTA) (Particle Metrix, North Carolina, USA). The morphology of EVs was observed using a JEM1400 transmission electron microscope (TEM, Hitachi, Tokyo, Japan). Western blot analysis was performed to detect the expression of EV surface marker proteins CD9 (1:1000, ab307085, Abcam), CD63 (1:1000, ab315108, Abcam), and the negative control Calnexin (1:1000, ab22595, Abcam). Conditioned media were obtained after adding the EV inhibitor GW4869 (10 μM; Sigma-Aldrich, St. Louis, MO, USA) to the cell culture medium according to the manufacturer's instructions. These media were labeled as the GW group.

### Co-immunoprecipitation (Co-IP)

Cells were lysed in IP lysis buffer (Pierce Biotechnology, Waltham, MA, USA), and protein concentrations were quantified using a BCA kit (Invitrogen, Waltham, MA, USA). Equal amounts of protein were incubated overnight with the primary antibody against Rab27B (1:1000, ab317264, Abcam) at 4 °C. The complexes were then incubated overnight with Protein A agarose beads (Pierce

Biotechnology, Waltham, MA, USA) at 4 °C. After washing with IP lysis buffer, the immunoprecipitated complexes were resolved by SDS-PAGE and subsequently analyzed by Western blot assay for PD-L1 (1:1000, PA5-20343, Invitrogen).

#### Experimental animals

Male BALB/c-nu nude mice (4–6 weeks old) and immunocompetent C57BL/6 mice (male, 4–6 weeks old, Beijing Vital River Laboratory Animal Technology, Beijing, China) were housed under specific pathogen-free conditions with a 12-hour light/dark cycle. All animals had free access to food and water.

#### Establishment and handling of animal models

For the subcutaneous tumor model, stably expressed U251 cells (100 μL, $5 \times 10^6$ cells) were subcutaneously implanted into the dorsal region of nude mice. Tumors were allowed to grow until they reached a diameter of 1 cm. Tumor growth was monitored every 7 days and the longest (a) and shortest (b) diameters of the tumors were measured using calipers. Tumor volume was calculated using the formula $V = ab^2 \times 0.5$. Tumor growth curves were plotted, and all tumors did not exceed 1.5 cm in diameter. All mice were included in the study. Four weeks post-implantation, all mice were euthanized by intraperitoneal injection of pentobarbital (200 mg/kg). Tumors were then excised and weighed, and randomly selected tumors from each group ($n = 6$) were fixed in formaldehyde and embedded in paraffin. The remaining tumors were homogenized for further analysis.

For the in situ tumorigenesis model, GL261 cells ($1 \times 10^5$ cells per mouse) were intracranially injected into the brain of C57BL/6 mice. Next, using a stereotactic frame, a burr hole was created on the skull using a 0.7 mm drill bit, positioned 1.5 mm to the right and 1.5 mm rostrally from the bregma. Cells were injected into the brain at a depth of 3 mm using a non-coring needle (Hamilton 7804-04, 26s gauge, Small Hub RN needle, point style: 4, needle length: 2 inches, angle: 12). The burr hole was covered with bone wax, and the skin incision was sutured. Mice received buprenex (0.05 mg/kg) once directly after surgery and again 4–6 h post-surgery. Before surgery and 12–24 h post-surgery, mice received an intraperitoneal injection of meloxicam and were monitored for signs of pain. EVs were administered via the tail vein (100 μg) every three days, and anti-PD-L1 antibody (200 mg/kg) was administered every three days. Mice exhibiting signs of feeding difficulties, allodynia, or significant weight loss were euthanized by intraperitoneal injection of pentobarbital (200 mg/kg), and their survival status was recorded. Brain tissues were then extracted, and tumors were resected. A total of 60 mice were used for the in situ tumorigenesis model, with 12 mice randomly assigned to each group: Lv-NC group: GL261 cells infected with Lv-NC lentivirus; Lv-antagomiR group: GL261 cells infected with Lv-antagomiR lentivirus; Lv-NC + PD-L1 group: GL261 cells infected with Lv-NC lentivirus and treated with anti-PD-L1 antibody; Lv-antagomiR + PD-L1 group: GL261 cells infected with Lv-antagomiR lentivirus and treated with anti-PD-L1 antibody; Lv-antagomiR + PD-L1 + EVs group: GL261 cells infected with Lv-antagomiR lentivirus and treated with both anti-PD-L1 antibody and EVs. After tumor extraction, six tumors from each group were randomly selected for flow cytometry analysis, and the remaining six tumors were homogenized for RNA or protein expression analysis.

#### Immunohistochemistry (IHC)

Tumor sections were deparaffinized, hydrated, and incubated overnight at 4 °C with anti-Ki67 antibody (1:200, ab16667, Abcam). Then the sections were used for incubation with IgG (1:2000, ab205718, Abcam) for 2 h at 37 °C. After washing with PBS, the sections were developed using 3,3'-diaminobenzidine as the substrate and $H_2O_2$ as the catalyst. The sections were then mounted and examined under a microscope for analysis.

#### Statistical analysis

SPSS 21.0 statistical software (IBM SPSS Statistics, Armonk, NY, USA) and GraphPad Prism 8.0 software (GraphPad Software Inc., San Diego, CA, USA) were applied for statistical analysis and graphing. Initially, normality and homogeneity of variance tests were performed. Data met the criteria of normal distribution and homogeneity of variance. Comparisons between two groups were conducted using the *t*-test. Comparisons among multiple groups were analyzed using one-way or two-way analysis of variance (ANOVA), followed by Tukey's multiple comparisons test for post hoc analysis. $p < 0.05$ was considered statistically significant.

## Results

#### Rab27B expression is reduced in glioma tissues

Our previous study showed downregulated LINC01018 and upregulated miR-182-5p in glioma [8]. Database prediction analysis of downstream targets of miR-182-5p indicated that Rab27B was downregulated in glioblastoma (Fig. 1A). Building upon these findings, we expanded our clinical sample size and further evaluated the expression of LINC01018, miR-182-5p, and Rab27B. Both LINC01018 and Rab27B were significantly downregulated in tumor tissues of glioblastoma patients ($p < 0.01$, Fig. 1B-C), whereas miR-182-5p was upregulated in tumor tissues ($p < 0.01$, Fig. 1B). Additionally, negative correlations were observed between the expression of LINC01018 and miR-182-5p and between

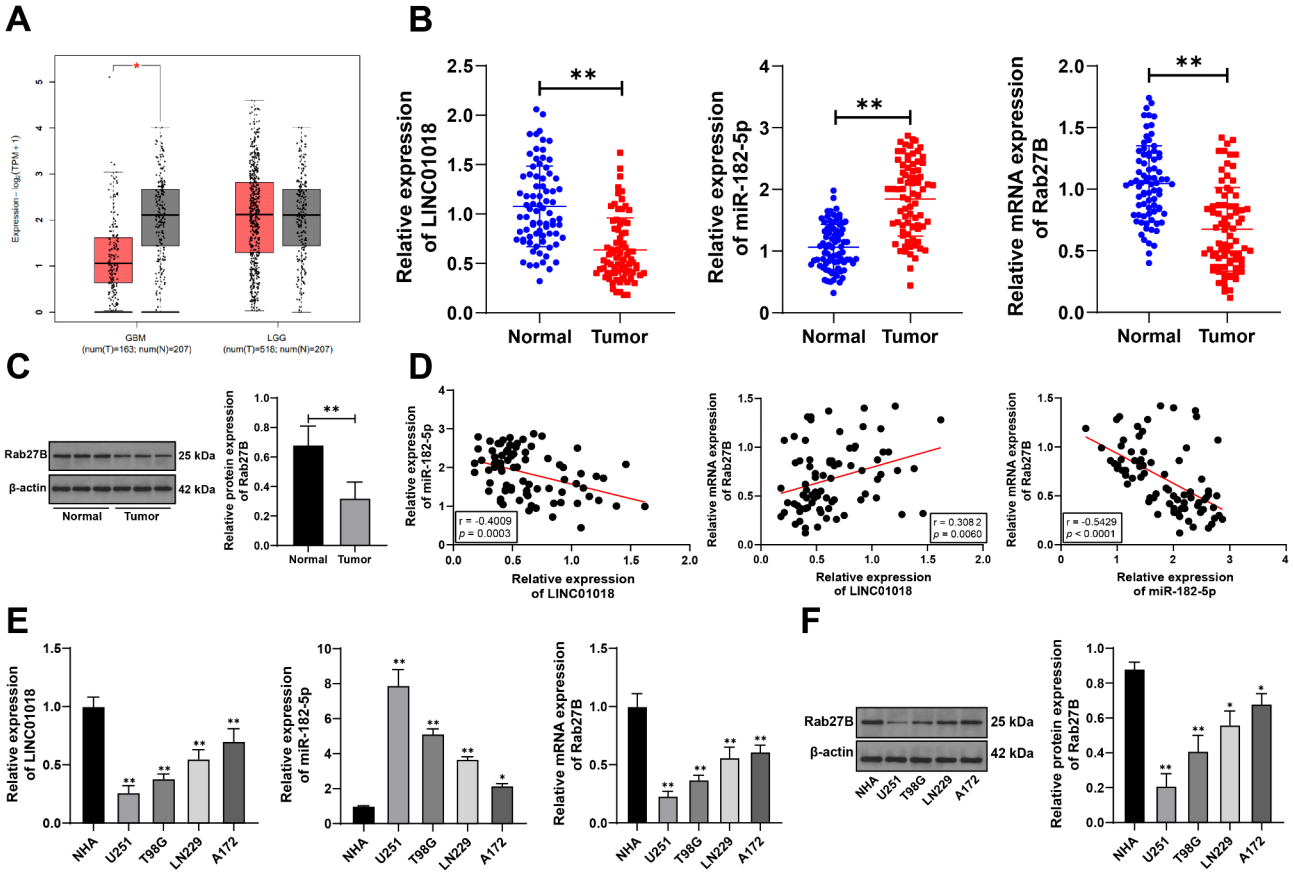


**Fig. 1** Rab27B expression is reduced in glioma tissues. **A**: Rab27B expression in GBM (Glioblastoma multiforme) and LGG (Brain Lower Grade Glioma) was predicted online using the GEPIA2 database (http://gepia2.cancer-pku.cn/#index) [34]. **B**: qRT-PCR was performed to detect the expression of LINC01018, miR-182-5p, and Rab27B in tumor tissues and adjacent normal tissues from 78 glioblastoma patients. **C**: Western blot analysis was conducted to assess the expression of Rab27B in tumor tissues and adjacent normal tissues from 78 glioblastoma patients, with representative band images shown. **D**: Pearson correlation analysis was performed to evaluate the correlation between the expressions of LINC01018, miR-182-5p, and Rab27B. **E**: qRT-PCR was used to measure the expression of LINC01018, miR-182-5p, and Rab27B in NHA and human glioma cell lines (U251, T98G, LN229, A172). with cell experiment repeated three times. **F**: Western blot analysis was employed to determine the expression of Rab27B in NHA and human glioma cell lines (U251, T98G, LN229, A172), with the experiment repeated three times. In panels **B** and **C**, ** $p < 0.01$; In panels **E** and **F**, * versus NHA, $p < 0.05$, ** versus NHA, $p < 0.01$. Data comparison between two groups in panels **B** and **C** was analyzed using *t*-test, and multiple group comparison in panels **E** and **F** was analyzed using one-way ANOVA, followed by Tukey's multiple comparisons test

miR-182-5p and Rab27B, while a positive correlation was found between LINC01018 and Rab27B expression ($p < 0.01$, Fig. 1D). Further examination within glioma cell lines revealed consistent expression patterns of LINC01018, miR-182-5p, and Rab27B as observed in the tissue samples ($p < 0.01$, Fig. 1E-F).

### LINC01018/miR-182-5p targets Rab27B expression

Dual-luciferase reporter assay showed that co-transfection with miR-182-5p mimic and Rab27B-WT suppressed luciferase activity within the system ($p < 0.01$, Fig. 2A). In previous studies, we overexpressed LINC01018 in U251 and T98G cells and conducted combined experiments by further overexpressing miR-182-5p [8]. Overexpression of LINC01018 significantly increased Rab27B expression ($p < 0.01$, Fig. 2B-C). However, after miR-182-5p was additionally overexpressed, Rab27B expression was decreased again ($p < 0.01$, Fig. 2B-C). These results suggest that LINC01018/miR-182-5p targets and regulates Rab27B expression.

### Rab27B inhibition reverses the inhibitory effects of overexpressed LINC01018 on proliferation and metastasis of glioma cells

We inhibited Rab27B expression within the cells ($p < 0.01$, Fig. 3A, D) and then conducted combined experiments with LINC01018 overexpression. Compared to LINC01018 overexpression alone, the combined group exhibited increased cell viability ($p < 0.01$, Fig. 3B), enhanced cell invasion and migration ($p < 0.01$, Fig. 3C), decreased E-cadherin expression, and increased N-cadherin and Vimentin expression ($p < 0.01$, Fig. 3D). These findings indicate that inhibition of Rab27B partially reverses the inhibitory effects of LINC01018

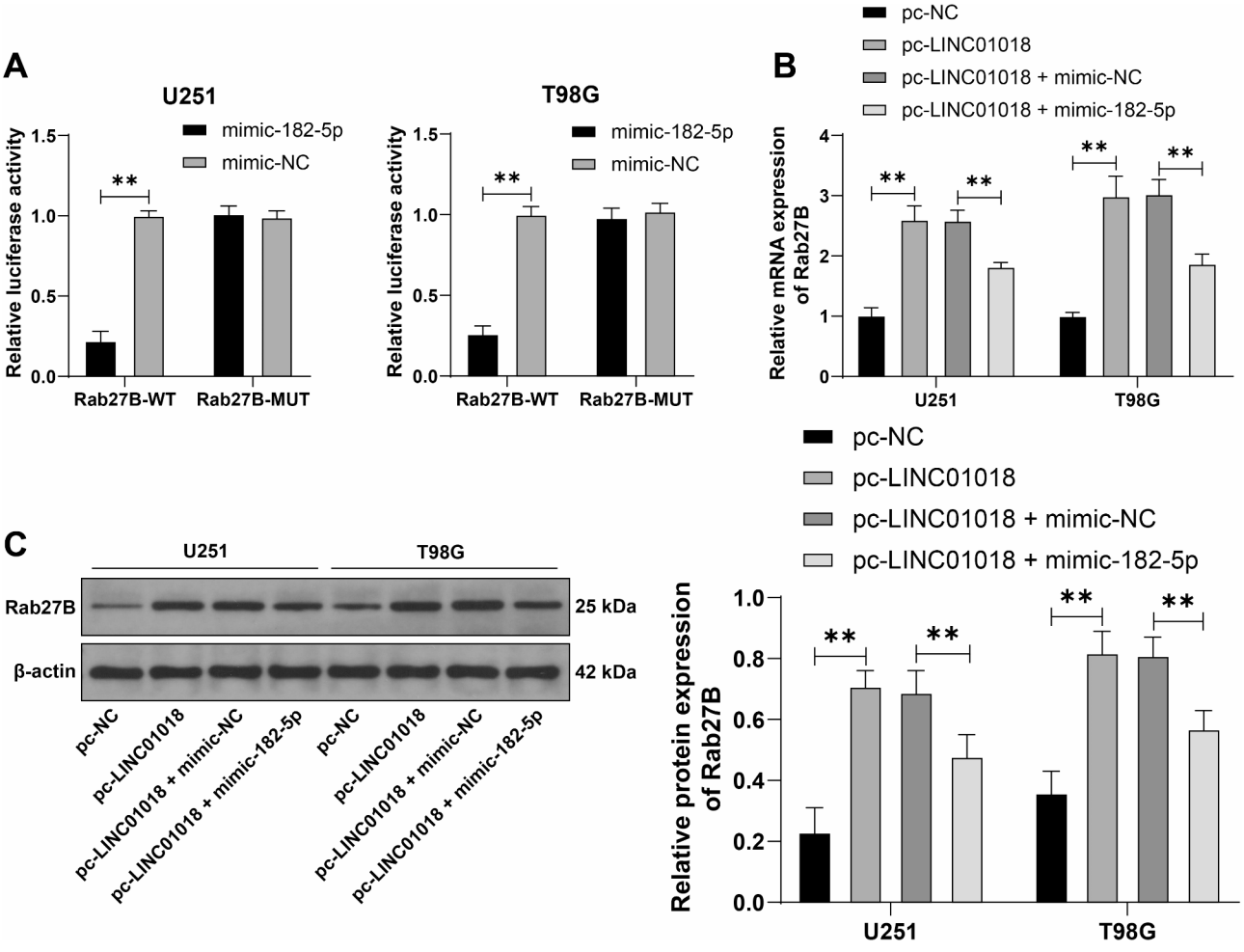


**Fig. 2** LINC01018/miR-182-5p targets Rab27B expression. **A**: Dual-luciferase reporter assays were conducted to investigate the binding relationship between miR-182-5p and Rab27B. **B**-**C**: The expression of Rab27B in U251 and T98G cells under different treatments was assessed using qRT-PCR and Western blot. The cell experiments were repeated three times. ** $p < 0.01$. Comparison of data was analyzed using two-way ANOVA, followed by Tukey's multiple comparisons test

overexpression on the proliferation and migration of glioma cells.

### Overexpression of LINC01018 suppresses glioma growth via the miR-182-5p/Rab27B axis

We established a xenograft model in nude mice by subcutaneous injection. Compared to the control group, glioma cells overexpressing LINC01018 exhibited significantly reduced tumor volume ($p < 0.01$, Fig. 4A), decreased tumor weight ($p < 0.01$, Fig. 4B), and reduced ki67 positivity within the tumors ($p < 0.01$, Fig. 4C). miR-182-5p was decreased and LINC01018 and Rab27B were increased in the Lv-LINC01018 group ($p < 0.01$, Fig. 4D-E). These findings suggest that overexpression of LINC01018 inhibits glioma growth through the miR-182-5p/Rab27B axis.

### Rab27B is involved in immune evasion of glioma cells

Furthermore, flow cytometry was conducted for the proportions of infiltrating macrophages and monocytes in patient tissues (Supplementary Fig. 1). Glioblastoma patients were allocated to high-Rab27B ($n = 39$) and low-Rab27B ($n = 39$) groups based on the median of the relative expression of Rab27B mRNA. The results showed that the low-Rab27B expression group had a higher percentage of macrophages and monocytes within the tumor tissues ($p < 0.01$, Fig. 5A-B). Although there was no significant difference in the proportion of $CD8^+$ T cells between the two groups ($p > 0.05$, Fig. 5C), the function of $CD8^+$ T cells within the tumors of the low-Rab27B expression group was suppressed, as indicated by elevated TIM-3 levels and significantly decreased IFN-γ expression ($p < 0.01$, Fig. 5D-E). The low-Rab27B expression group exhibited higher PD-L1 expression ($p < 0.01$, Fig. 5F). These results suggest a potential association of Rab27B with immune evasion in glioma.

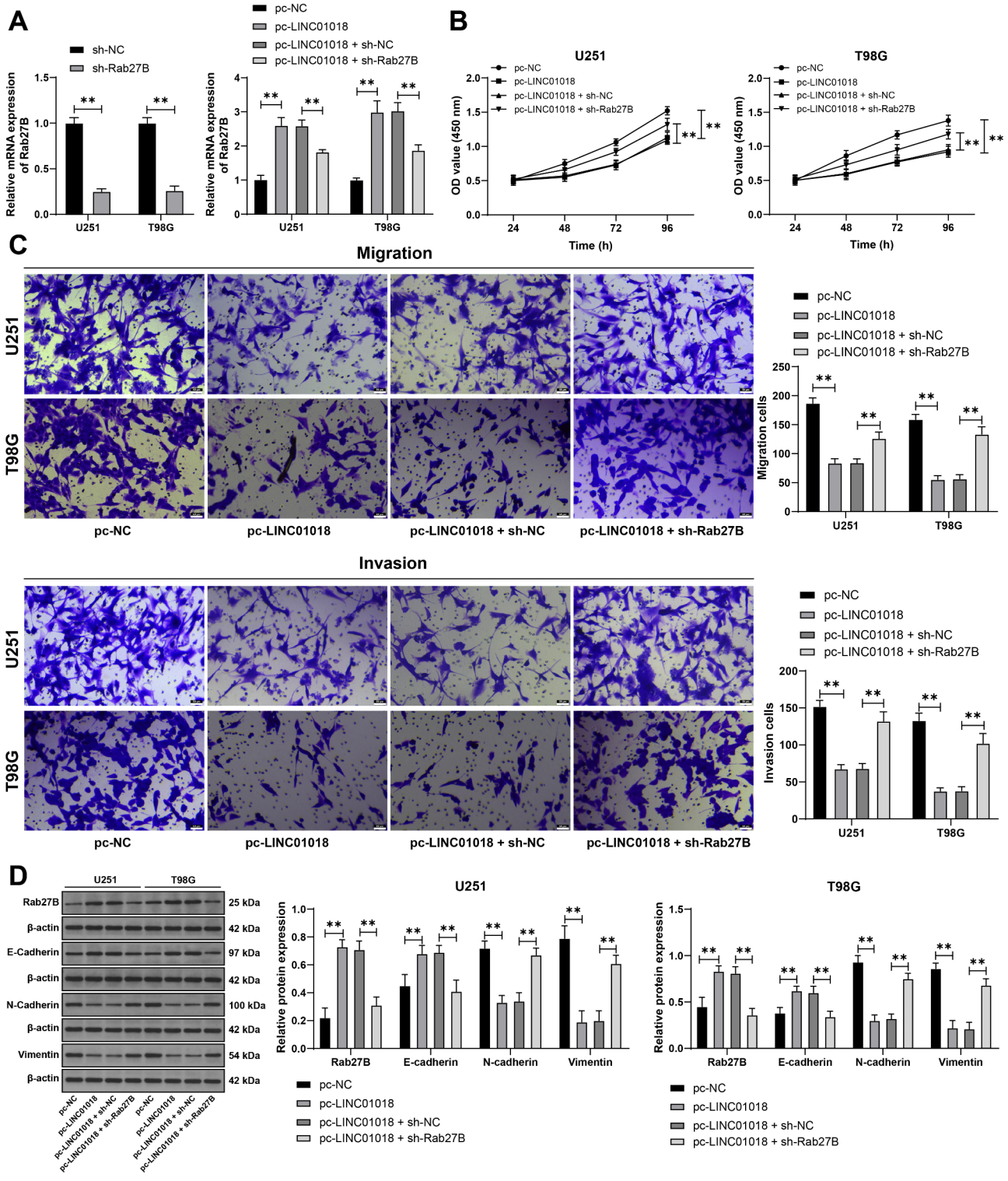


**Fig. 3** Rab27B inhibition reverses the inhibitory effects of overexpressed LINC01018 on proliferation and metastasis of glioma cells. sh-Rab27B was transfected into U251 and T98G cells, with sh-NC as a control, followed by combined experiments with LINC01018 overexpression. **A**: qRT-PCR was performed to detect the expression of Rab27B in the cells. **B**: Cell viability was assessed using CCK-8 assay. **C**: Transwell assay was used to evaluate cell invasion and migration. **D**: Western blot analysis was conducted to measure the expression of Rab27B, E-cadherin, N-cadherin, and Vimentin in the cells. The cell experiments were repeated three times. ** $p < 0.01$. Comparison of data was analyzed using two-way ANOVA, followed by Tukey's multiple comparisons test

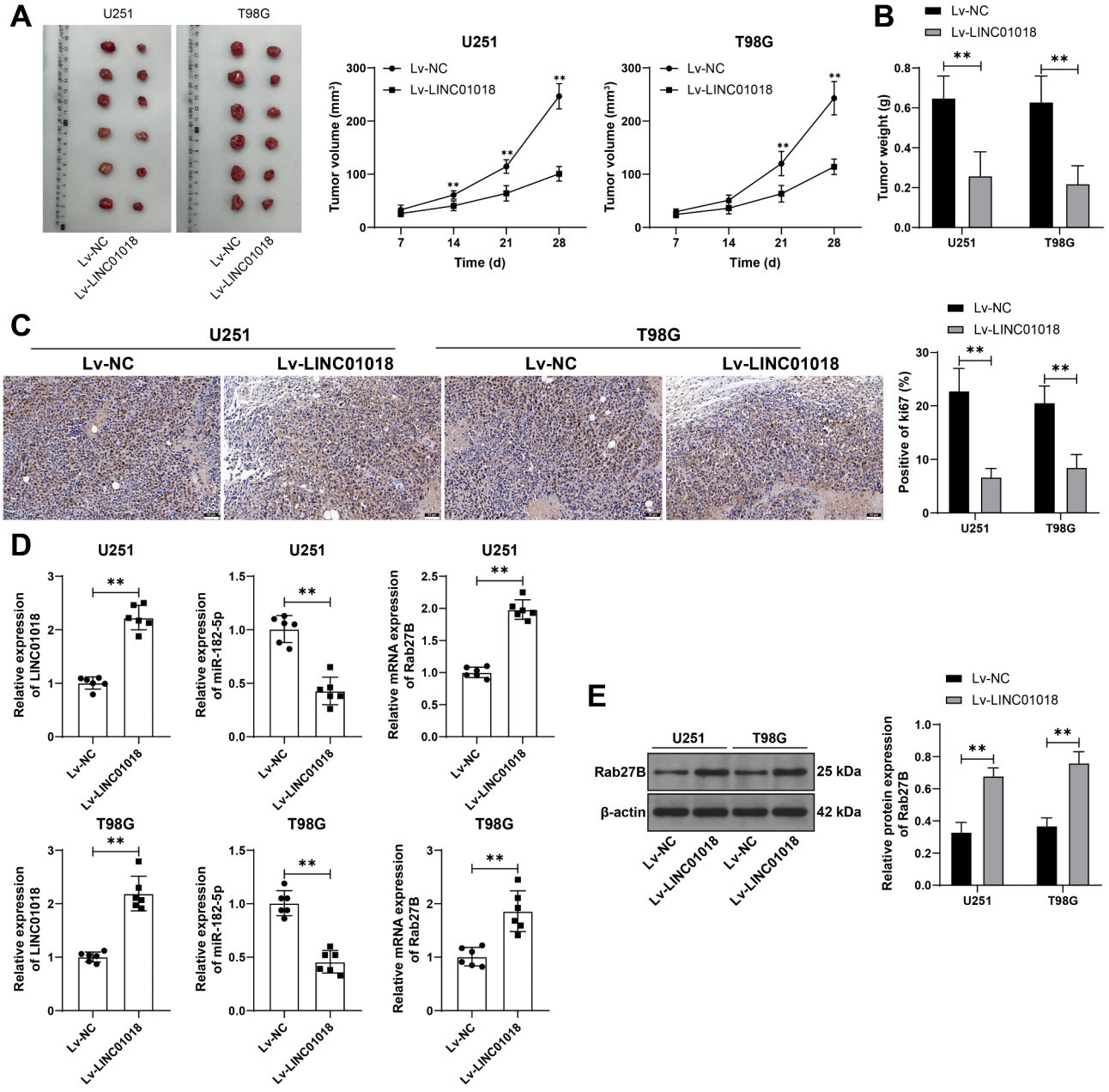


**Fig. 4** Overexpression of LINC01018 suppresses glioma growth via the miR-182-5p/Rab27B axis. Glioma cells (U251, T98G) with stable overexpressed LINC01018 (Lv-LINC01018) was generated by lentiviral infection, with Lv-NC as the control. These stably expressing cells were subcutaneously injected into nude mice. **A**: Tumor volume was measured every 7 days, and the tumors were harvested after 28 days when the mice were euthanized. $N=12$. **B**: Tumor weight was recorded. $N=12$. **C**: IHC was performed to assess the expression of ki67 in the tumors. $N=6$. **D**: qRT-PCR was used to detect the expression of LINC01018, miR-182-5p, and Rab27B in the tumors. $N=6$. **E**: Western blot analysis was conducted to measure the expression of Rab27B in the tumors. $N=6$. ** $p<0.01$. Comparison of data in panels **A**, **B**, **C**, and **E** was analyzed using two-way ANOVA, followed by Tukey's multiple comparisons test; data in panel **D** were analyzed using *t*-test

### The LINC01018/miR-182-5p/Rab27B axis is involved in the transport of PD-L1 in glioma cell-derived EVs

Initially, we purified EVs from the supernatant of U251 cells and validated them through TEM and NTA. The majority of EVs were within the typical size range of 30–150 nm (Supplementary Fig. 2A-B). Furthermore, Western blot analysis of the EV markers CD9 and CD63, as well as the negative marker Calnexin, confirmed the successful isolation of EVs (Supplementary Fig. 2C). Immunoprecipitation demonstrated the binding of Rab27B to PD-L1 in both cells and EVs (Fig. 6A). Rab27B inhibition significantly increased PD-L1 expression in EVs ($p<0.01$, Fig. 6B). Overexpression of LINC01018 significantly reduced PD-L1 expression in EVs, which

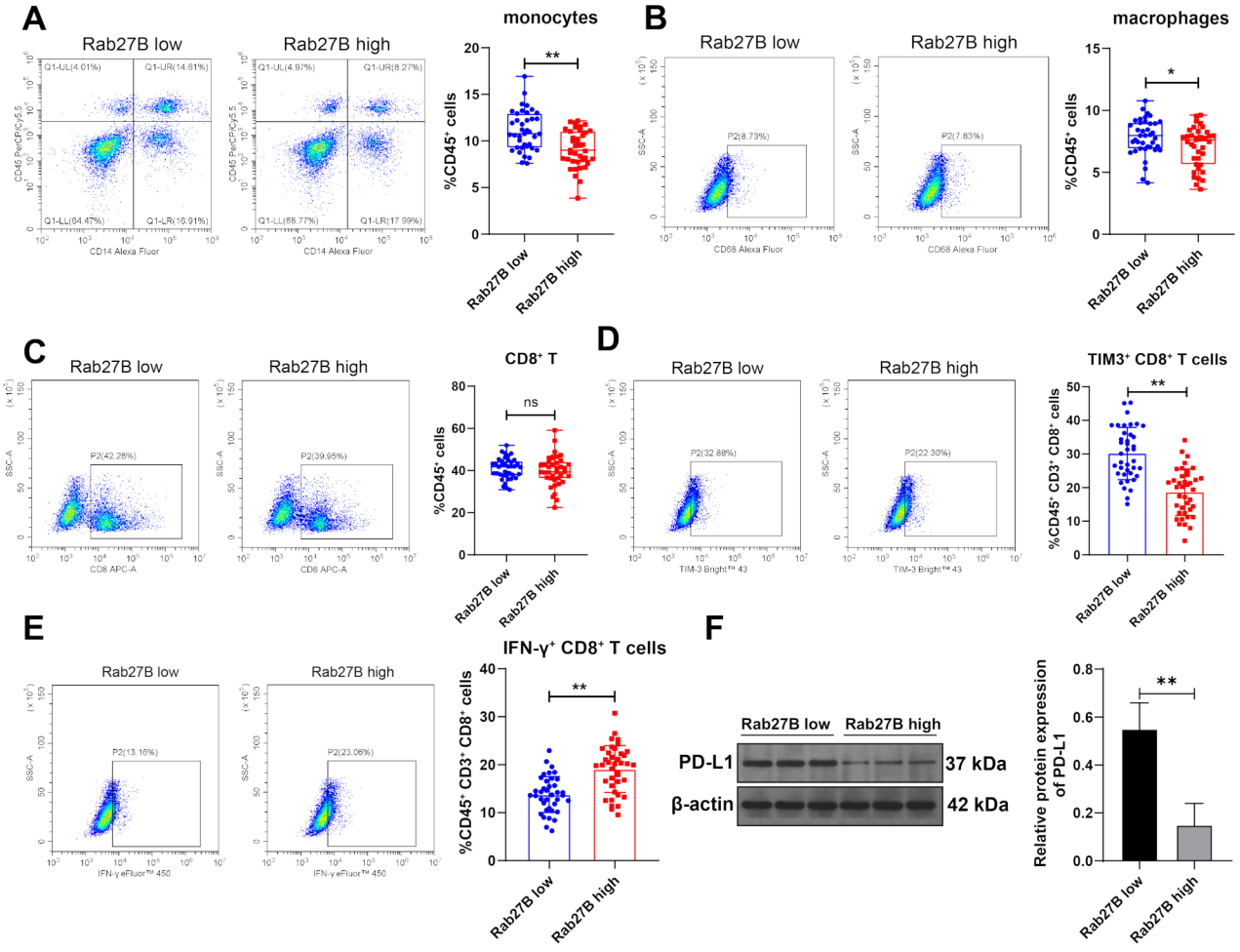


**Fig. 5** Rab27B is involved in immune evasion of glioma cells. Glioblastoma patients were divided into high expression group ($n=39$) and low expression group ($n=39$) based on the expression of Rab27B. **A**-**C**: The proportions of monocytes ($CD45^+CD14^+$), macrophages ($CD45^+CD14^+CD68^+$), and $CD8^+$ T cells ($CD45^+CD3^+CD8^+$) in each glioma tissue were analyzed by flow cytometry. **D**-**E**: The functional status of $CD8^+$ T cells was analyzed by flow cytometry. **F**: Western blot was performed to detect the expression of PD-L1 in the tissues. ns $p>0.05$, * $p<0.05$, ** $p<0.01$. Data were analyzed using *t*-test, with representative band images shown

was reversed upon miR-182-5p overexpression ($p<0.01$, Fig. 6B). In contrast, there was no significant difference in PD-L1 expression within cells. However, Rab27B inhibition did not affect EV release (no significant difference in EV concentration and marker protein expression from an equal amount of glioma cell-derived EVs) ($p<0.01$, Fig. 6C). These results indicate that the LINC01018/miR-182-5p/Rab27B axis is involved in regulating the transport of PD-L1 in glioma cell-derived EVs.

### Glioma cell-derived EVs deliver PD-L1 and increase PD-L1 expression in microglia

Subsequently, we co-cultured glioma cells (U251, T98G) with HMC3 cells and observed an increase in PD-L1 expression in microglia. However, the addition of an EV inhibitor did not significantly alter PD-L1 expression ($p<0.01$, Fig. 7A). Furthermore, we assessed the transfer of EV cargo from glioma cells to microglia using the CreLoxP system. EVs were isolated from cells transfected with Rab27B-Cre and then microglial cells were transfected with a pLV-CMVLoxP-DsRed-Stop-LoxP-eGFP virus. Following transfection, the fluorescence of microglia was red, with no detectable green fluorescence (Fig. 7B). Subsequently, upon the addition of the previously extracted EVs to microglia, the red fluorescence turned green, indicating that Rab27B-Cre derived-EVs were absorbed by microglia, and their cargo functioned within the microglia (Fig. 7B). Furthermore, PD-L1 was upregulated in microglia following EV treatment, while EVs overexpressing LINC01018 reduced PD-L1 expression ($p<0.01$, Fig. 7C). Additionally, EV treatment significantly increased the level of the M2 marker CD206

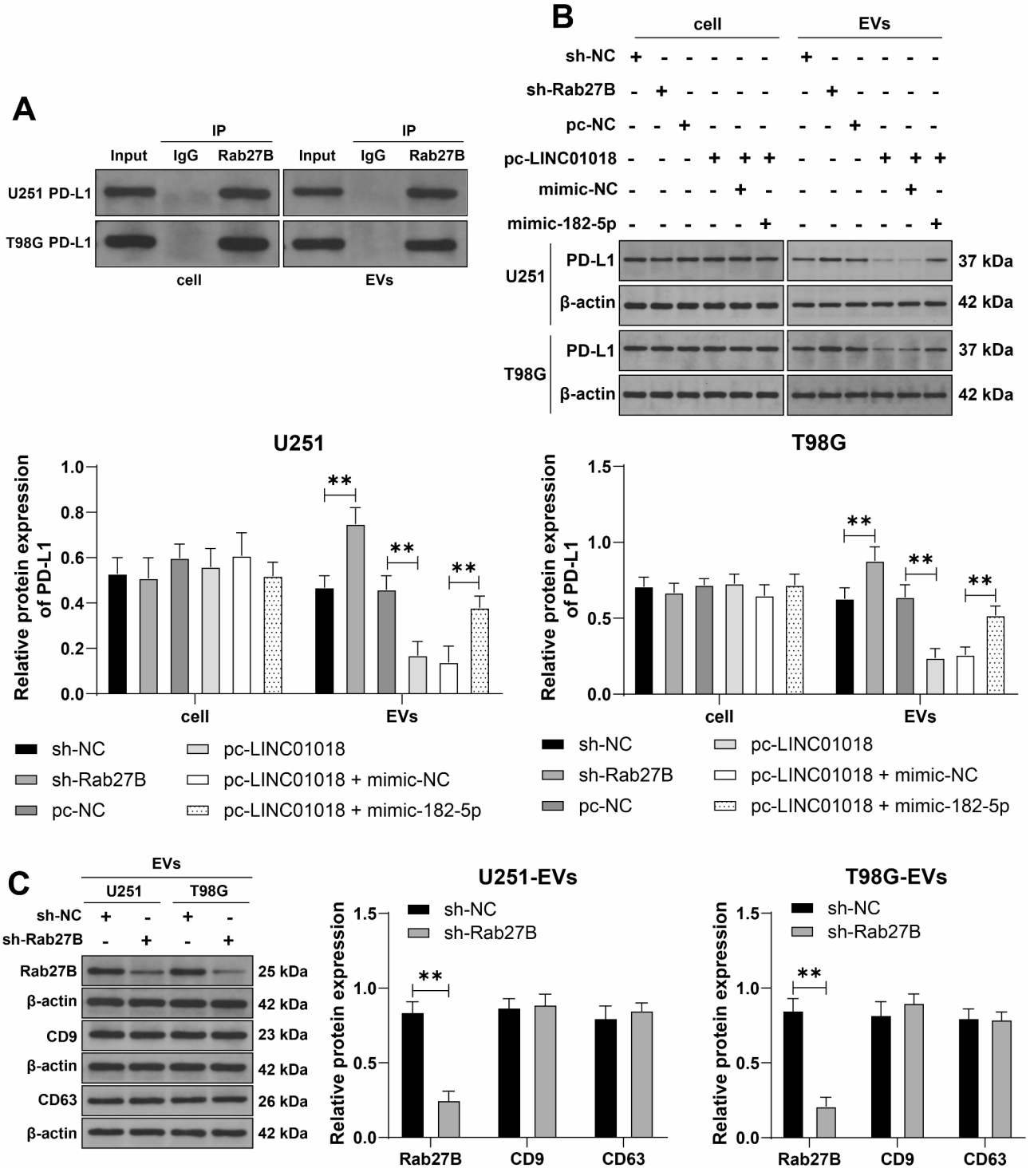


**Fig. 6** The LINC01018/miR-182-5p/Rab27B axis is involved in the transport of PD-L1 in glioma cell-derived EVs. **A**: Immunoprecipitation was performed to detect the binding of Rab27B to PD-L1 in cells and EVs. **B**: Western blot was conducted to measure the expression of PD-L1 in cells and EVs. **C**: Western blot was used to detect the expression of Rab27B, CD9, and CD63 in EVs. The cell experiments were repeated three times. $^{**}p < 0.01$. Data in panels **B** and **C** were analyzed using two-way ANOVA, followed by Tukey's multiple comparisons test

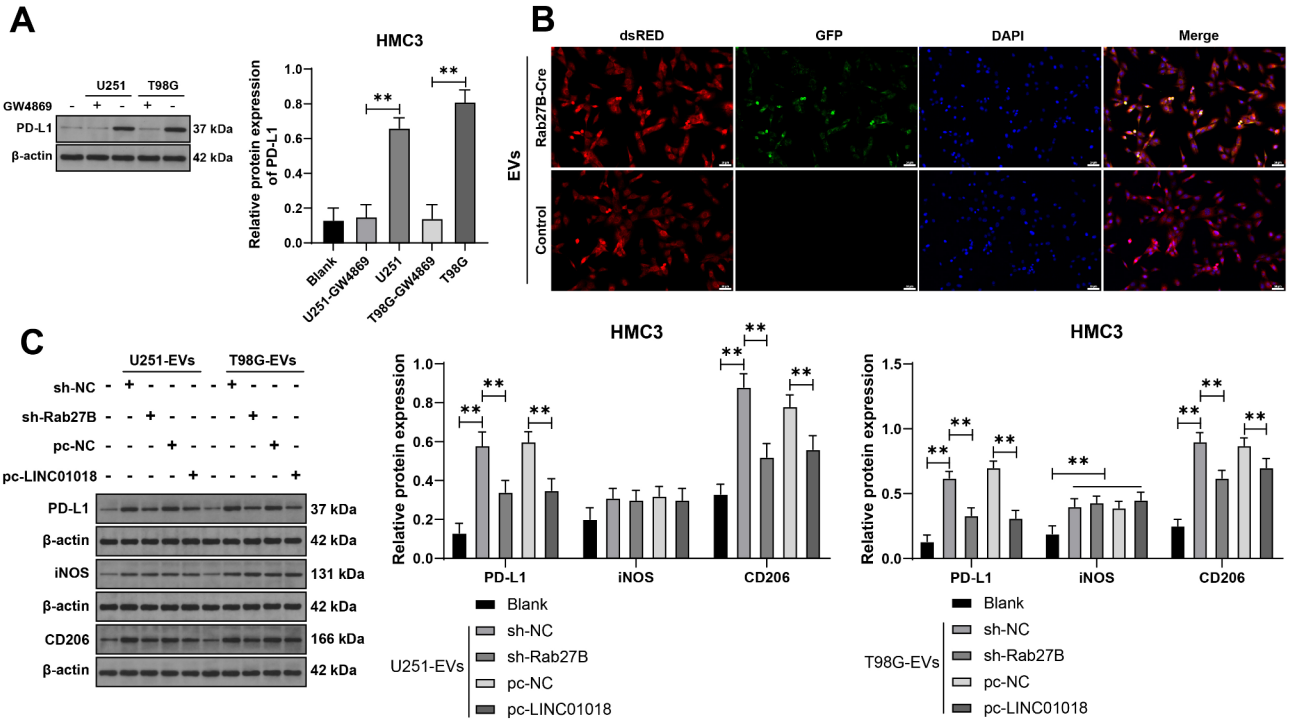


**Fig. 7** Glioma cell-derived EVs delivery PD-L1 and increase PD-L1 expression in microglial cells. **A**: Glioma cells (U251, T98G) with or without GW4869 were co-cultured with human microglial cells HMC3, and the expression of PD-L1 in HMC3 cells after co-culture was detected by Western blot. **B**: The CreLoxP system was used to evaluate the delivery of EV cargo from glioma cells to microglial cells. **C**: Western blot was used to detect the expression of PD-L1, iNOS and CD206 in HMC3 cells treated with different EVs. The cell experiments were repeated three times. ** $p < 0.01$. Data were analyzed by two-way ANOVA, followed by Tukey's multiple comparisons test.

in microglia ($p < 0.01$, Fig. 7C). These results suggest that EVs from glioma cells increase PD-L1 expression in microglia through cargo delivery and influence the M1/M2 differentiation of microglia.

### Rab27B mediates glioma cell-derived EVs to regulate PD-L1 transfer and promote immune escape in vivo

We established an orthotopic glioma model in C57BL/6 mice by injecting GL261 cells and treated them with anti-PD-L1. The results showed that inhibition of miR-182-5p increased Rab27B expression in the tumor ($p < 0.01$, Fig. 8A-B) and enhanced the therapeutic effect of anti-PD-L1, resulting in a significant increase in the survival rate of the mice ($p < 0.01$, Fig. 8C). However, the survival rate decreased after injection of EVs ($p < 0.01$, Fig. 8C). miR-182-5p inhibition markedly reduced macrophages and infiltrating TAMs ($p < 0.01$, Fig. 8D, Supplementary Fig. 3), while their levels increased after EVs injection ($p < 0.01$, Fig. 8D, Supplementary Fig. 3). Consistent with the findings in human tumors, miR-182-5p inhibition did not significantly affect $CD8^+$ T cells in the tumor, while anti-PD-L1 therapy increased the number and function of $CD8^+$ T cells in the tumor ($p < 0.05$, Fig. 8D-E, Supplementary Fig. 3). EV injection significantly upregulated PD-L1 expression in the tumor ($p < 0.01$, Fig. 8F). These results indicate that Rab27B mediates glioma-derived EVs to regulate PD-L1 transfer and promotes immune escape of glioma cells in vivo.

## Discussion

Glioma possesses a unique immune microenvironment characterized by the infiltration of two types of immune cells: microglia and TAMs, primarily of the M2 phenotype, which engage in antigen presentation and secrete various inflammatory factors [19]. Our main findings indicate that in glioma, the LINC01018/miR-182-5p/Rab27B axis promoted the M2 polarization of microglia by regulating the transport of PD-L1 via glioma cell-derived EVs, thereby facilitating the immune escape of glioma cells (Fig. 9).

Based on our previous research, the LINC01018/miR-182-5p/Rab27B axis may be a critical pathway involved in the proliferation and metastasis of glioma cells [8]. Our present study showed that overexpression of LINC01018 significantly increased Rab27B expression, while subsequent overexpression of miR-182-5p led to a decrease in Rab27B expression. Here, Rab27B was lowly expressed in glioma cancer tissues and enhances cell invasion and migration. In addition, low expression of Rab27B enhances the proliferation and invasion of nasopharyngeal carcinoma cells, thereby increasing their radioresistance [20]. Interestingly, Rab27B activation promotes the

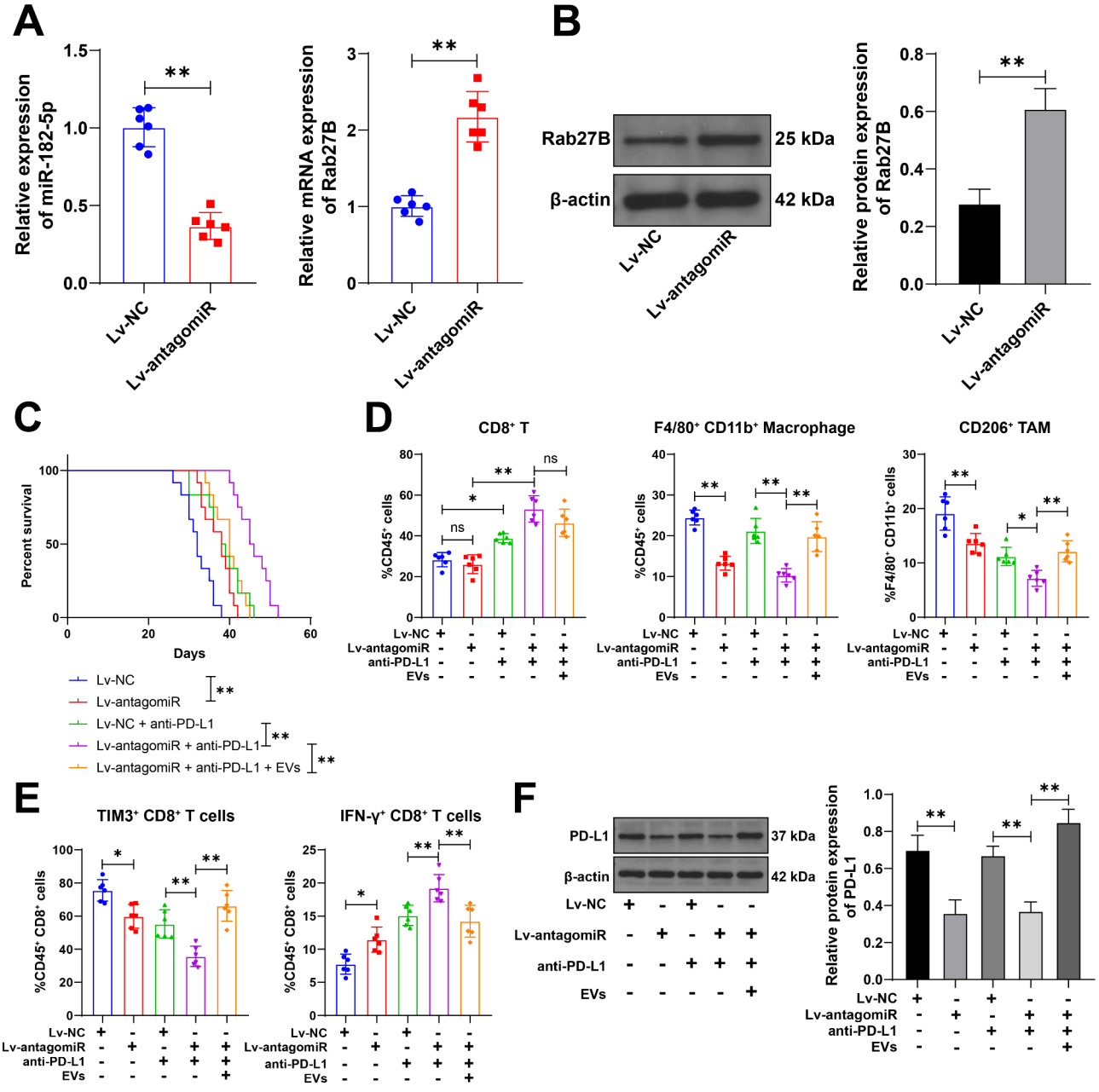


**Fig. 8** Rab27B mediates glioma cell-derived EVs to regulate PD-L1 transfer and promotes immune escape in vivo. The GL261 cells with stable low expression of miR-182-5p (Lv-antagomiR) were injected into mice, with Lv-NC serving as the control. Anti-PD-L1 treatment was administered every 3 days along with intravenous injection of glioma cell-derived EVs. **A**: qRT-PCR was conducted to detect the expression of miR-182-5p and Rab27B in the tumor, $n=6$; **B**: Western blot was performed to assess Rab27B expression in the tumor, $n=6$; **C**: Survival status of mice in different treatment groups was recorded, $n=12$; **D**: Flow cytometry was used to determine the proportions of $CD8^+$ T cells ($CD45^+CD8^+$), macrophages ($CD45^+F4/80^+CD11b^+$), and TAM ($F4/80^+$ $CD11b^+$ $CD206^+$) in the tissues, $n=6$; **E**: The functional status of $CD8^+$ T cells was analyzed by flow cytometry, $n=6$; **F**: Western blot was utilized to measure PD-L1 expression in the tumor, $n=6$; ns $p>0.05$, * $p<0.05$, ** $p<0.01$. Data in panels **A** and **B** were analyzed by *t*-test; data in panels **D**, **E**, and **F** were analyzed by one-way ANOVA analysis, followed by Tukey's multiple comparisons test

secretion of exosomes from colorectal cancer stem cells, contributing to an immunosuppressive microenvironment by increasing the number of $CD66^+$ neutrophils and decreasing the number of $CD8^+$ T cells [21]. Cytotoxic $CD8^+$ T cells can regulate immune signals, provide protective immunity, and eliminate malignant cells [22]. In the diffuse intrinsic pontine glioma, TIM-3 is highly expressed in microglia in tumor microenvironment, while blocking TIM-3 can enhance the levels of T cells, NK cells, and trigger pro-inflammatory chemokines, exerting anti-tumor effects [23]. Elevating IFN-γ levels in glioma cells may increase the proliferation and cytotoxic

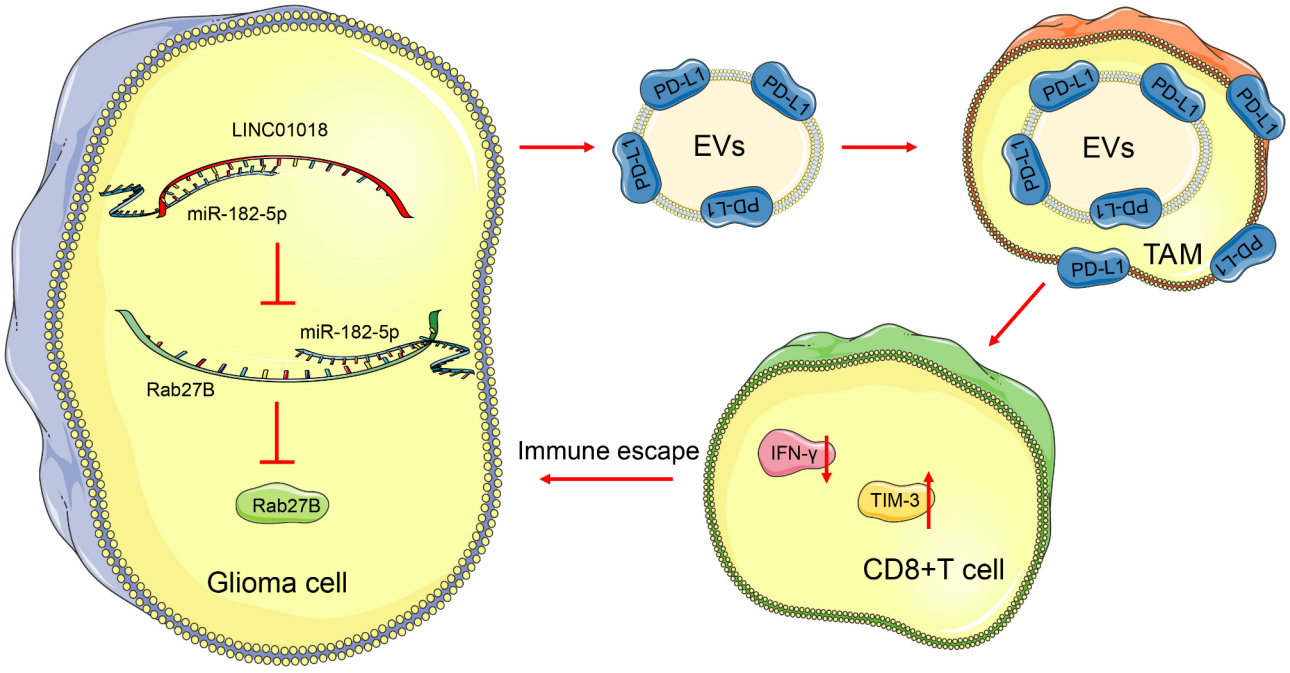


**Fig. 9** LINC01018 is downregulated in glioma cells. LINC01018 promotes the transport of PD-L1-carrying EVs into microglia and increases PD-L1 expression through the miR-182-5p/Rab27B axis, inhibiting $CD8^+$ T cell function and promoting immune evasion in glioma cells

activity of $CD8^+$ T cells, thereby blocking immune evasion [24]. The degradation of PD-L1 in gliomas increases T lymphocytes and promotes T cell infiltration, reshaping the tumor immune microenvironment [25]. Our study suggested that in glioblastoma patients with low expression of Rab27B, $CD8^+$ T cell function was suppressed, TIM-3 level was upregulated, IFN-γ was remarkedly downregulated, and PD-L1 was highly expressed. Moreover, in hepatocellular carcinoma, Rab27B knockdown promotes the transfer of PD-L1 to EVs, inducing the suppression of $CD8^+$ T cells and leading to immune escape of cancer cells [10]. Herein, we propose that downregulation of Rab27B may promote immune escape of glioma cells by inhibiting the function of $CD8^+$ T cells in clearing tumor cells.

Further research found that inhibiting Rab27B significantly increased PD-L1 expression in glioma cell-derived EVs without affecting the release of EVs. PD-L1 levels in EVs are significantly higher in cancer patients compared to healthy individuals, and anti-PD-L1 therapy can induce antitumor immunity [26]. In the early stages of glioma, PD-L1 accumulates on microglia and binds to PD-1, leading to M2 polarization of microglia within the glioma microenvironment, which promotes tumor growth and invasion [27]. PD-L1 in glioblastoma-derived-EVs markedly suppress T cell activation [28]. Meanwhile, PD-L1 inhibition and the M2 polarization of macrophages can effectively alleviate the immunosuppressive tumor microenvironment in glioma [29]. In our research, we found that miR-182-5p inhibition significantly reduced macrophages and infiltrating TAMs in the tumor and enhanced the therapeutic effect of anti-PD-L1, which was reversed by glioma cell-derived EVs delivering PD-L1. Another study consistently demonstrated that miR-182-5p inhibitor reduced the expression of PD-L1 transcripts in triple-negative breast cancer [30]. miR-182-5p can directly induce T-cell dysfunction in cancer cells [31] and modulate the immune response in the tumor microenvironment by impacting immune cell involvement [32]. miR-182-5p directly targets and reduces factors associated with T cell activation and proliferation, impairing the immune response [33]. We verified that PD-L1 expression in EVs was regulated by the miR-182-5p/Rab27B axis. Anti-PD-L1 treatment restored the function of $CD8^+$ T cells.

Our study has several limitations. Firstly, the tumor immunosuppressive microenvironment involves numerous immune cells, including $CD8^+$ T, $CD3^+$ T cells, natural killer cells, natural killer T cells, macrophages, monocytes, and myeloid-derived suppressor cells, whose complex functions have not been fully validated in our study. Secondly, LINC01018 is currently known to be expressed only in humans, and we cannot directly manipulate LINC01018 expression in murine cells when performing xenograft tumor formation experiments. Thirdly, we did not conduct H&E and IHC analysis of the orthotopic tumors to compare the histological characteristics and protein expression. Fourthly, the primary cell culture that is closer to the original state of human tumors has not been carried out yet. Lastly, other downstream

targets of the LINC01018/miR-182-5p axis have not yet been validated. In the future, we will expand our clinical sample size to further investigate the role of other downstream targets of the LINC01018/miR-182-5p axis in glioma development and immune escape, aiming to provide new insights for improving treatment resistance and identifying new therapeutic targets.

In conclusion, upon our previous findings that the LINC01018/miR-182-5p axis can regulate Rab27B expression, this study further elucidates that Rab27B promotes the carriage of PD-L1 by glioma cell-derived EVs into microglia, thereby increasing PD-L1 expression on TAMs, suppressing $CD8^+$ T cell function, and facilitating the immune escape of glioma cells.

## Supplementary Information

The online version contains supplementary material available at https://doi.org/10.1186/s13062-025-00651-w.

Supplementary Material 1

Supplementary Material 2

Supplementary Material 3

Supplementary Material 4

**Acknowledgements**
Not applicable.

**Author contributions**
S H: Conceptualization, Data curation, Formal analysis, Writing—original draft. GS C: Writing—original draft. AP L: Investigation, Data Curation. HL Z: Investigation, Writing-review & Editing. D L: Methodology, Formal Analysis. B P: Investigation. JK D: Supervision, Project administration. DD L: Conceptualization, Funding acquisition, Supervision.

**Funding**
This work was supported by the Guangdong Province Medical Science and Technology Research Fund (A2024087).

**Data availability**
No datasets were generated or analysed during the current study.

## Declaration

**Ethics approval and consent to participate**
The study protocol adhered to the ethical guidelines of ethics committee of Guangzhou Institute of Cancer Research, the Affiliated Cancer Hospital, Guangzhou Medical University and the Declaration of Helsinki. All animal experiments were approved by the ethics committee of Guangzhou Institute of Cancer Research, the Affiliated Cancer Hospital, Guangzhou Medical University and conducted in accordance with the Guide for the Care and Use of Laboratory Animals [16]

**Consent for publication**
Not applicable.

**Competing interests**
The authors declare no competing interests.

**Author details**
[1]Department of Neurosurgery, Guangzhou Institute of Cancer Research, the Affiliated Cancer Hospital, Guangzhou Medical University, Guangzhou 510095, China
[2]Department of Intervention, the Affiliated Cancer Hospital, Guangzhou Institute of Cancer Research, Guangzhou Medical University, Guangzhou 510095, China
[3]Department of Radiology, the Affiliated Cancer Hospital, Guangzhou Institute of Cancer Research, Guangzhou Medical University, Guangzhou 510095, China
[4]Department of Medical Oncology, Guangzhou Institute of Cancer Research, the Affiliated Cancer Hospital, Guangzhou Medical University, Guangzhou 510095, China

Received: 25 December 2024 / Accepted: 15 April 2025
Published online: 21 May 2025

**References**

1. Weller M, Wen PY, Chang SM, Dirven L, Lim M, Monje M, Reifenberger G, Glioma. Nat Rev Dis Primers. 2024;10(1):33.
2. Xu S, Tang L, Li X, Fan F, Liu Z. Immunotherapy for glioma: current management and future application. Cancer Lett. 2020;476:1–12.
3. Yasinjan F, Xing Y, Geng H, Guo R, Yang L, Liu Z, Wang H. Immunotherapy: a promising approach for glioma treatment. Front Immunol. 2023;14:1255611.
4. Wang C, Chen Q, Chen M, Guo S, Hou P, Zou Y, Wang J, He B, Zhang Q, Chen L, et al. Interaction of glioma-associated microglia/macrophages and anti-PD1 immunotherapy. Cancer Immunol Immunother. 2023;72(6):1685–98.
5. Bridges MC, Daulagala AC, Kourtidis A. LNCcation: LncRNA localization and function. J Cell Biol. 2021;220(2).
6. Entezari M, Taheriazam A, Orouei S, Fallah S, Sanaei A, Hejazi ES, Kakavand A, Rezaei S, Heidari H, Behroozaghdam M, et al. LncRNA-miRNA axis in tumor progression and therapy response: an emphasis on molecular interactions and therapeutic interventions. Biomed Pharmacother. 2022;154:113609.
7. Xu J, Wang J, Zhao M, Li C, Hong S, Zhang J. LncRNA LINC01018/miR-942-5p/KNG1 axis regulates the malignant development of glioma in vitro and in vivo. CNS Neurosci Ther. 2023;29(2):691–711.
8. Su H, Hailin Z, Dongdong L, Jiang Y, Shuncheng H, Shun Z, Dan L, Biao P. Long non-coding RNA LINC01018 inhibits human glioma cell proliferation and metastasis by directly targeting miRNA-182-5p. J Neurooncol. 2022;160(1):67–78.
9. Izumi T. In vivo roles of Rab27 and its effectors in exocytosis. Cell Struct Funct. 2021;46(2):79–94.
10. Chen J, Lin Z, Liu L, Zhang R, Geng Y, Fan M, Zhu W, Lu M, Lu L, Jia H, et al. GOLM1 exacerbates CD8(+) T cell suppression in hepatocellular carcinoma by promoting Exosomal PD-L1 transport into tumor-associated macrophages. Signal Transduct Target Ther. 2021;6(1):397.
11. Tankov S, Walker PR. Glioma-Derived extracellular Vesicles - Far more than local mediators. Front Immunol. 2021;12:679954.
12. Soraya H, Sani NA, Jabbari N, Rezaie J. Metformin increases exosome biogenesis and secretion in U87 MG human glioblastoma cells: A possible mechanism of therapeutic resistance. Arch Med Res. 2021;52(2):151–62.
13. Kornepati AVR, Vadlamudi RK, Curiel TJ. Programmed death ligand 1 signals in cancer cells. Nat Rev Cancer. 2022;22(3):174–89.
14. Tang Q, Chen Y, Li X, Long S, Shi Y, Yu Y, Wu W, Han L, Wang S. The role of PD-1/PD-L1 and application of immune-checkpoint inhibitors in human cancers. Front Immunol. 2022;13:964442.
15. Zhang H, Liu L, Liu J, Dang P, Hu S, Yuan W, Sun Z, Liu Y, Wang C. Roles of tumor-associated macrophages in anti-PD-1/PD-L1 immunotherapy for solid cancers. Mol Cancer. 2023;22(1):58.
16. Guide for the Care and Use of Laboratory Animals. The National Academies Collection: Reports funded by National Institutes of Health. 8th ed. Washington (DC)2011.
17. Nong W, Bao C, Chen Y, Wei Z. miR-212-3p attenuates neuroinflammation of rats with Alzheimer's disease via regulating the SP1/BACE1/NLRP3/Caspase-1 signaling pathway. Bosn J Basic Med Sci. 2022;22(4):540–52.
18. Livak KJ, Schmittgen TD. Analysis of relative gene expression data using real-time quantitative PCR and the 2(-Delta Delta C(T)) method. Methods. 2001;25(4):402–8.
19. Guo X, Wang G. Advances in research on immune escape mechanism of glioma. CNS Neurosci Ther. 2023;29(7):1709–20.
20. Huang D, Bian G, Pan Y, Han X, Sun Y, Wang Y, Shen G, Cheng M, Fang X, Hu S. MiR-20a-5p promotes radio-resistance by targeting Rab27B in nasopharyngeal cancer cells. Cancer Cell Int. 2017;17:32.

21. Cheng WC, Liao TT, Lin CC, Yuan LE, Lan HY, Lin HH, Teng HW, Chang HC, Lin CH, Yang CY, et al. RAB27B-activated secretion of stem-like tumor exosomes delivers the biomarker microRNA-146a-5p, which promotes tumorigenesis and associates with an immunosuppressive tumor microenvironment in colorectal cancer. Int J Cancer. 2019;145(8):2209–24.
22. Reina-Campos M, Scharping NE, Goldrath AW. CD8(+) T cell metabolism in infection and cancer. Nat Rev Immunol. 2021;21(11):718–38.
23. Ausejo-Mauleon I, Labiano S, de la Nava D, Laspidea V, Zalacain M, Marrodan L, Garcia-Moure M, Gonzalez-Huarriz M, Hervas-Corpion I, Dhandapani L, et al. TIM-3 Blockade in diffuse intrinsic Pontine glioma models promotes tumor regression and antitumor immune memory. Cancer Cell. 2023;41(11):1911–26. e8.
24. Yang F, Wang T, Du P, Fan H, Dong X, Guo H. M2 bone marrow-derived macrophage-derived exosomes shuffle microRNA-21 to accelerate immune escape of glioma by modulating PEG3. Cancer Cell Int. 2020;20:93.
25. Tang W, Xu N, Zhou J, He Z, Lenahan C, Wang C, Ji H, Liu B, Zou Y, Zeng H, et al. ALKBH5 promotes PD-L1-mediated immune escape through m6A modification of ZDHHC3 in glioma. Cell Death Discov. 2022;8(1):497.
26. Mishra S, Amatya SB, Salmi S, Koivukangas V, Karihtala P, Reunanen J. Microbiota and extracellular vesicles in Anti-PD-1/PD-L1 therapy. Cancers (Basel). 2022;14(20).
27. Wang XP, Guo W, Chen YF, Hong C, Ji J, Zhang XY, Dong YF, Sun XL. PD-1/PD-L1 axis is involved in the interaction between microglial polarization and glioma. Int Immunopharmacol. 2024;133:112074.
28. Ricklefs FL, Alayo Q, Krenzlin H, Mahmoud AB, Speranza MC, Nakashima H, Hayes JL, Lee K, Balaj L, Passaro C, et al. Immune evasion mediated by PD-L1 on glioblastoma-derived extracellular vesicles. Sci Adv. 2018;4(3):eaar2766.
29. Chen T, Liu J, Wang C, Wang Z, Zhou J, Lin J, Mao J, Pan T, Wang J, Xu H et al. ALOX5 contributes to glioma progression by promoting 5-HETE-mediated immunosuppressive M2 polarization and PD-L1 expression of glioma-associated microglia/macrophages. J Immunother Cancer. 2024;12(8).
30. Samir A, Tawab RA, El Tayebi HM. Long non-coding RNAs XIST and MALAT1 hijack the PD-L1 regulatory signaling pathway in breast cancer subtypes. Oncol Lett. 2021;22(2):593.
31. Cui J, Li Q, Luo M, Zhong Z, Zhou S, Jiang L, Shen N, Geng Z, Cheng H, Meng L, et al. Leukemia cell-derived microvesicles induce T cell exhaustion via MiRNA delivery. Oncoimmunology. 2018;7(7):e1448330.
32. Lei T, Zhang Y, Wang X, Liu W, Feng W, Song W. Integrated analysis of the functions and clinical implications of exosome circrnas in colorectal cancer. Front Immunol. 2022;13:919014.
33. Soheilifar MH, Vaseghi H, Seif F, Ariana M, Ghorbanifar S, Habibi N, Papari Barjasteh F, Pornour M. Concomitant overexpression of mir-182-5p and mir-182-3p raises the possibility of IL-17-producing Treg formation in breast cancer by targeting CD3d, ITK, FOXO1, and NFATs: A meta-analysis and experimental study. Cancer Sci. 2021;112(2):589–603.
34. Tang Z, Kang B, Li C, Chen T, Zhang Z. GEPIA2: an enhanced web server for large-scale expression profiling and interactive analysis. Nucleic Acids Res. 2019;47(W1):W556–60.


## Publisher's note